JOURNAL OF APPLIED ELECTROCHEMISTRY 17 (1987) 1203–1212

Double-layer capacitance and polarization potential of baked carbon anodes in cryolite–alumina melts

STANISLAW JAREK*, JOMAR THONSTAD

Laboratories of Industrial Electrochemistry, Norwegian Institute of Technology, University of Trondheim, 7034 Trondheim-NTH, Norway

Received 2 December 1986; revised 18 June 1987

Baked carbon anodes with varying apparent densities and baking temperatures were tested in Na_3AlF_6–$Al_2O_{3(sat)}$ melts at 1010° C. The double-layer capacitance (C_{dl}) was used as an indicator of the wetted surface area. For unpolarized anodes, C_{dl} increased with increasing time of immersion and reached a constant level after 1.5–2 h. The values decreased with increasing polarization potential in the range 1–1.5 V positive to aluminium. The C_{dl} of polished samples increased markedly during electrolysis, particularly at low current densities. No clear correlation was found between C_{dl} and apparent density. Semi-logarithmic plots of potential versus current could be divided into three segments. The lower two were linear, the ranges and slopes being 0.01–0.1 A cm^{-2}, 0.20–0.44 V per decade and 0.1–0.5 A cm^{-2}, 0.18–0.24 V per decade, respectively. At higher current densities the curves bent upwards. The current density corresponding to an overpotential of 0.5 V increased slightly with increasing apparent density, whereas the ohmic voltage drop at constant current density decreased. The current densities were corrected for differences in wetted surface area on the basis of the C_{dl} data. The change in baking temperature from 970 to 1100° C had no appreciable effect on the overpotential, whereas samples baked at 1250° C showed a somewhat lower overpotential.

1. Introduction

The polarization potential of carbon anodes in cryolite–alumina (Na_3AlF_6–Al_2O_3) melts has been measured by many workers [1]. It is determined by the rate of the anodic part of the cell reaction

$$Al_2O_3 + \tfrac{3}{2}C = 2Al + \tfrac{3}{2}CO_2 \qquad (1)$$

which involves the discharge of oxygen-containing ions and the oxidation of the carbon anode yielding CO_2. The published data on polarization potential show large variations [1], and it is not clear to what extent the scatter is due to different porosity, i.e. different wetted surface area, and to what extent it is due to different reactivity of the tested materials. Experimental factors may be equally important, such as grain distribution, anode size, edge effects, etc.

Carbon anodes are made of amorphous petroleum coke and pitch binder (~ 20 wt %). The petroleum coke is produced in the delayed coking process and precalcined at ~ 1300° C. The tar pitch binder is calcined during baking of the compacted anode. The reactivity of the binder phase depends on the baking temperature. The porosity of the anodes depends mainly on the porosity of the filler coke, the compacting technique and the baking temperature. High porosity offers a large working surface area of the anode, which for a given current density (referred to the apparent surface area) should give a lower polarization potential compared to a denser material. Likewise, high reactivity is expected to give a low polarization potential, since reaction overpotential is a part of it [1].

Despite the significance of the effect of porosity, systematic studies in this field are scarce. Dumas and Brenet [2] determined the polarization potential on different types of

* *Present address*: Hydro Aluminium, R & D Carbon, 5875 Ardalstangen, Norway.

0021-891X/87 $03.00 + .12

Table 1. Processing details and properties of the baked carbon anodes used

Compacting method	*Mixing temperature (° C)*	*Forming pressure (kPa cm^{-2})*	*Forming time (s)*	*Baking temperature (° C)*	*Apparent density (g cm^{-3})*
Pressing for 1 min	140	160		970	1.32
	140	130			1.35
	120	–			1.42
	150	130		1000	1.42
	160	120			1.48
	170	160			1.58
Vibration under 50 kPa cm^{-2}	165		10	1250	1.56
			20		1.59
			60		1.61

carbonaceous materials with varying BET surface area (s_{BET}). A linear relationship between the polarization potential of the anodes and ln s_{BET} was found empirically, in the sense that a high s_{BET} corresponded to a low potential. Sverdlin *et al.* [3] found no relationship between the counter electromotive force (e.m.f.) and the total porosity of carbon anodes, while the counter e.m.f. was found to decrease with increasing pore volume in the 26–73 μm size range. Zuca *et al.* [4, 5] correlated electrochemical properties of baked carbon with microporosity for pores larger than 7.5 μm. The Tafel range, the Tafel slope and the critical current density (for the initiation of the anode effect) were found to decrease with increasing microporosity, whereas the exchange current density and the ohmic voltage drop increased. Thus, the decrease in overpotential with increasing porosity was partly offset by an increase in ohmic voltage drop.

In situ assessment of the wetted surface area of baked carbon anodes is essential in order to study the effect of porosity. Measurement of the double-layer capacitance (C_{dl}) appears to be the best method for this purpose. It can be assumed that C_{dl} will be proportional to the area which is wetted by the melt, i.e. the electroactive surface area. This assumption was adopted in the present study, and C_{dl} was used as an indirect measure of the wetted surface area. Anodes made of industrial quality carbon having different apparent densities and baked at different temperatures were compared. The influence on C_{dl} of polarization potential, soaking time and electrolytic consumption was studied, followed by steady-state polarization measurements.

2. Preparation of anodes

The anode materials were prepared at the Carbon Laboratory of Hydro Aluminium at Ardalstangen. The green paste was fabricated from industrial grade petroleum coke (mean crystallite size, L_c = 3.1 nm) and coal tar pitch (16.7 wt %) with a softening point of 104° C (Mettler). The paste was either pressure molded or vibratory compacted into blocks. The mixing temperature, forming conditions and baking temperatures were varied to obtain samples with different apparent densities, i.e. by varying porosity. The anodes were machined from drilled cores of this material. Table 1 summarizes processing parameters and the properties of these baked cores. The apparent density of the cores was determined on a mass–volume basis. In addition, microporosity for 0.01–70 μm diameter was measured by the mercury pressure porosimetry method. It should be noted that the lowest apparent densities given in Table 1 are well below the normal range of apparent densities used in industry (1.5–1.6 g cm^{-3}). The lowest baking temperature corresponds to that of Soderberg anodes.

The cores with low apparent density, especially those baked at 970° C, had a rough surface, and macropores could easily be seen. The cores baked at 1250° C had a smoother appearance and a more uniform micropore size distribution,

as reported elsewhere [6]. However, even in this case both apparent density and microporosity showed significant variations even for cores taken from the same carbon block. In general, no correlation was found between apparent density and microporosity.

3. Double-layer capacitance

3.1. *Experimental details*

The cell was contained in a graphite crucible which also served as cathode. The melt consisted of natural Greenland cryolite (Na_3AlF_6) saturated with alumina (~ 14 wt % Al_2O_3) at 1010 $\pm$ 2° C. The cylindrical anode (21–22 mm) was shaped as a hemisphere at the end. The sides were shielded by a boron nitride sheath so that only the hemispherical part was exposed to the melt, the geometrical surface area being $\sim 7\,cm^2$. An anode of this size was assumed to be statistically representative because the maximum size of individual particles of the petroleum coke aggregate did not exceed 5.6 mm. Separate leads for current and for potential measurements were embedded in the anode. An aluminium reference electrode was housed in an alumina tube with a hole (~ 0.5 mm) in the side facing the anode. The cell was placed in a gas-tight furnace under nitrogen atmosphere.

The C_{dl} was determined by means of an a.c. technique using a Solartron Schlumberger 1250 Frequency Response Analyzer. The impedance of the carbon anodes was normally measured against the aluminium reference electrode. A typical Nyquist diagram for baked anode at potential 1.2 V is shown in Fig. 1. The real part (Z_r) of the measured impedance decreased with increasing frequency, usually attaining a constant level in the range 8–20 kHz; it tended to increase slightly again at higher frequencies. An average value for Z_r within the constant range was taken as the ohmic resistance of the electrolyte. The inductance of the circuit was determined from the imaginary part (Z_j) at frequencies above 20 kHz. After correction for the inductance and the electrolyte resistance, R_{el}, the series system ($R_s C_s$) was converted into the equivalent parallel system ($R_p C_p$). The average value of C_p within the high-frequency range,

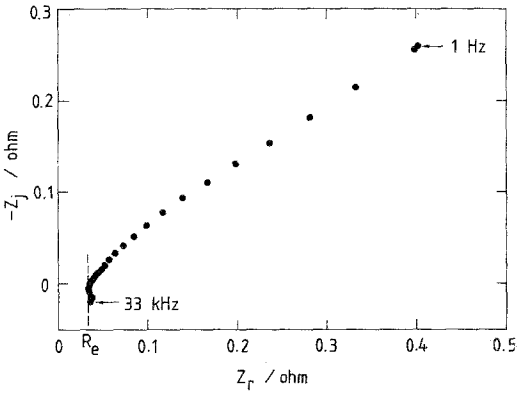

Fig. 1. A typical Nyquist diagram for baked carbon at 1.2 V in Na_3AlF_6–Al_2O_3 melt at 1010° C. Anode properties: apparent density, 1.5 g cm^{-3}; baking temperature, 1250° C.

where it attained a constant level, was taken as C_{dl}. The range of frequencies where C_{dl} attained a stable level was sometimes narrow and it varied from one sample to the other, probably due to the high and unevenly distributed porosity of the samples. Since both C_{dl} and R_{el} were evaluated from high-frequency impedance data, the majority of the measurements was carried out within the 3.5–65.5 kHz range.

Except for a series of experiments where the effect of potential was studied, C_{dl} was determined at a polarization potential of 1.2 V positive to aluminium. At this slightly anodic potential, disturbances at the interface due to gas evolution were avoided. When the effect of the time of immersion (soaking) was studied, the electrodes were kept at the zero current potential, which varied from 0.6 to 0.9 V, except for the short periods of time (~ 2 min) needed for the impedance measurements when the anode potential was set to 1.2 V.

The hemispherical anode was not suited for the study of changes in C_{dl} when carbon was consumed during electrolysis, because the geometrical surface area diminished during electrolysis. Similar to a design used previously [7], the anode was then prepared with a flat working surface (30 mm in diameter) shielded by boron nitride, and was positioned almost vertically with a slight inclination to ensure uniform wear. Before electrolysis the surface was carefully polished with alumina paste to a mirror-like finish. The graphite crucible served both as reference electrode in the a.c. circuit and as

cathode in this part of the work. It was found that the C_{dl} values were not affected by the absence of the aluminium reference electrode. To improve reproducibility the anodes were conditioned by pre-electrolysis at $2\,A\,cm^{-2}$ for 30 s. After the initial C_{dl} had been determined at 1.2 V the anodes were electrolysed at constant current density in the range $0.2-2.4\,A\,cm^{-2}$. The C_{dl} was determined five times during each run after passage of a charge of $\sim 0.7\,A\,h\,cm^{-2}$ each time. For the C_{dl} measurements the potential was set temporarily at 1.2 V. The total anode consumption corresponded to a layer approximately 2.5 mm thick. In one experiment a 3-mm rod of non-porous vitreous carbon was used as the working electrode.

3.2. *Results and discussion*

The curvature of the Nyquist plot in Fig. 1 at high frequencies represents the double-layer capacitance in parallel with the charge transfer resistance. At decreasing frequency the plot reaches the linear portion which represents diffusion impedance. Detailed analysis of the impedance spectra was beyond the scope of this work. A large scatter of C_{dl} values obtained in preliminary tests indicated that, among other factors, the C_{dl} might be dependent on the residence time of the anodes in the electrolyte. The changes in C_{dl} with the soaking time of baked carbon and vitreous carbon are shown in Fig. 2. No aluminium was present in the crucible during these measurements. The rate of the initial increase of C_{dl} varied from one specimen to the other, but in all cases it reached a constant level after 1.5–2 h. This level probably corresponds to penetration of open pores in the proximity of the surface. Correspondingly, the ohmic resistance of the cell (R_{el}) showed an initial decrease towards a stable level. Microscopic examination of used anodes showed the presence of frozen bath inside the pores at a distance of up to 1 cm from the working surface.

Literature data on C_{dl} of baked carbon anodes show large variations. In one work Thonstad [8] found C_{dl} to vary from 150 to $600\,\mu F\,cm^{-2}$, the average being $350\,\mu F\,cm^{-2}$, independent of current density within the range $0-0.15\,A\,cm^{-2}$. For another make of baked carbon an average

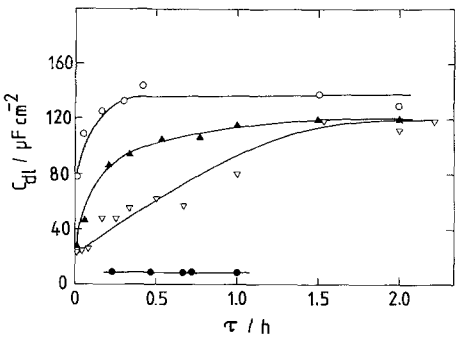

Fig. 2. Change of C_{dl} of unpolarized baked carbon during immersion time (τ) in Na_3AlF_6–Al_2O_3 melt at 1010° C. ○, △, ▽, the same type of baked carbon; ●, vitreous carbon.

value of $140\,\mu F\,cm^{-2}$, determined at 1.2 V, was found [7]. Jarek and Orman [9] reported a value of $104\,\mu F\,cm^{-2}$ for baked carbon at $0.05\,A\,cm^{-2}$. There is also considerable variation in C_{dl} data for graphite with values ranging from 10 to $100\,\mu F\,cm^{-2}$ [8–11]. This scatter probably reflects the inhomogeneity of the microstructure and the porosity, especially in the case of baked carbon. In aqueous solutions it has been found that even in the case of smooth carbon electrodes made of vitreous carbon or pyrolytic graphite, for example, C_{dl} is strongly dependent on the type of carbon and on the pretreatment of the electrode [12].

As shown in Fig. 2, the C_{dl} of the vitreous carbon anode ($\sim 9\,\mu F\,cm^{-2}$) did not change with the immersion time. Vetyukov and Akgva [13] reported $C_{dl} = 40\,\mu F\,cm^{-2}$ for vitreous carbon (at 1–1.1 V versus aluminium), while Thonstad [8] found it to be $9\,\mu F\,cm^{-2}$ at low anodic current density ($0.004-0.010\,A\,cm^{-2}$), in agreement with the present finding. It appears that the ratio of the wetted surface area of baked carbon to that of a non-porous material like vitreous carbon is at least 10.

The behaviour of C_{dl} for well-soaked carbon anodes (2 h) at varying polarization potential is illustrated in Fig. 3. Although the numerical values were poorly reproducible, the shape of the curves was similar for new as well as electrolysed anodes. A rapid increase of the capacitance when a cathodic current was flowing ($E < 1.1$ V) was also observed on vitreous carbon [7], and it was believed to be connected with specific adsorption of cations and discharged species. The C_{dl} seemed to approach a stable

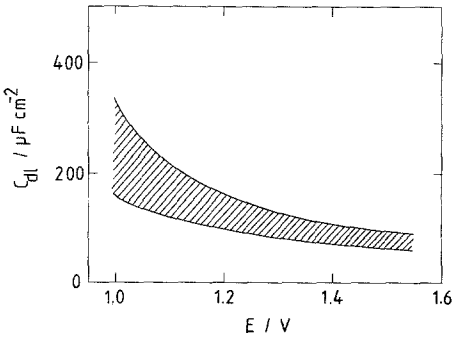

Fig. 3. The C_{dl} of baked carbon in Na_3AlF_6–Al_2O_3 melt at 1010° C versus potential referred to the aluminium electrode.

level at around 1.5–1.6 V. The decline of C_{dl} with increasing potential may be due to a true double-layer effect, but it may also be due to shielding of the surface by gas bubbles. Measurements at potentials above 1.4 V tended to be unreliable because of the high gas evolution rate. For vitreous carbon Vetyukov and Akgva [13] found a maximum in C_{dl} at ~ 1.27 V, while Thonstad [8] observed a steady increase, levelling off at above 1.2 V.

In previous work [7–10] the C_{dl} of baked carbon was found to increase during electrolysis. The change in C_{dl} as a percentage of the initial value is plotted versus the applied current density in Fig. 4, together with earlier results obtained for unpolished anodes after consumption of 2.5 mm of the anode [7]. Although the anodes were machined from the same carbon

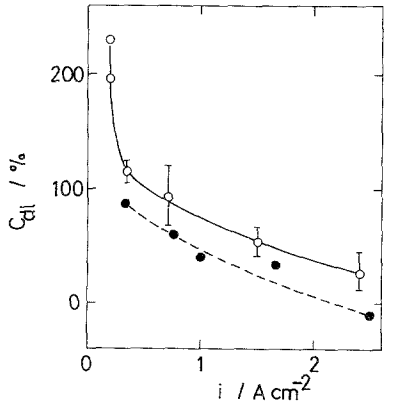

Fig. 4. Change of C_{dl} (% of initial value) of baked carbon anodes as a function of current density used during electrolysis at 1010° C corresponding to 2.5 mm consumption of the anodes. ○, Present work; ●, Thonstad [7].

Table 2. The double-layer capacitance of anodes with different apparent densities and baking temperatures

Baking temperature (° C)	*Apparent density (g cm^{-3})*	C_{dl} *(μF cm^{-2})*
970	1.32	220
	1.35	280
	1.42	220
1100	1.42	280
	1.48	250
	1.55	210
1250	1.56	225
	1.59	220
	1.61	230

block and polished in the same manner, the initial C_{dl} values varied from 130 to 350 μF cm^{-2}. The large increase of C_{dl} by electrolysis at low current densities can be attributed to roughening of the surface by selective consumption of the binder phase of the anode [1]. This was clearly evident by microscopic examination of used anodes. The height of the protrusions of aggregate coke was higher the lower the current density. This is in full agreement with earlier observations [14–16]. It is known from studies of gas reactivity (CO_2) that the binder phase is the more reactive part which is preferentially consumed. The fact that this is also the case during electrolysis supports the notion of a slow chemical reaction being the rate-determining step of the anode process [1]. As the current density is increased the preferential attack is suppressed because of the increased ohmic resistance term and because reaction in the pores is inhibited by the presence of gas bubbles. The idea of mass transfer limitation of the reaction in the pores at high current densities is supported by impedance measurements [8, 9].

Values of C_{dl} measured on anodes machined from cores with different apparent densities and different baking temperatures are given in Table 2. The data are averages of three measurements performed on the same sample before the polarization test. The variation in the assessment of C_{dl} for the same anode did not exceed 25 μF cm^{-2}, being in average less than 15 μF cm^{-2}. As before, C_{dl} is referred to the geometrical surface area. The results indicate that there is no clear

correlation between C_{dl} and apparent density of baking temperature. A change of apparent density by almost 0.3 g cm^{-3} for samples baked at 970 and 1250° C, did not result in any significant change in C_{dl}, although such a change would have been expected judging from the appearance of the materials. However, with all due reservations for the scatter of the results, a slight tendency of C_{dl} to decrease with increasing apparent density can be distinguished.

No clear relationship was found between C_{dl} and the cumulative pore volume in any of the three ranges: 0.01–70, 22–70 and 35–70 μm. The large scatter of C_{dl} and the lack of such correlation were probably due to the presence of larger pores not accessible for the microporosimeter and to a high overall structural non-uniformity of the materials, so that even two samples cut from the same core could be far from identical.

4. Polarization studies

4.1. *Experimental details*

The same cell and anodes were used as in the C_{dl} measurements. Prior to the polarization tests the anodes were conditioned by immersion in the melt for 1.5–2 h to avoid changes in surface area due to soaking and by the subsequent short pre-electrolysis (2 min at 2 A cm^{-2}). Then the C_{dl} was determined and current–voltage curves were recorded by potential increases in steps of 50 mV in the range from 1.2 V positive to aluminium to that corresponding to 10 A, which was the maximum output of the potentiostat (Wenking HP72). The duration of each step was 30 s, which was sufficient to attain steady state. A short cathodic depolarization (1 min at -0.1 A cm^{-2}) was applied before the potential steps were reversed. The ohmic resistance was determined by the impedance technique on applying superimposed a.c. at every second potential step. The resistance varied from 0.025 to 0.050 Ω depending on the type of anode and the current density. The precision of the resistance measurements was estimated to be 5×10^{-4} Ω.

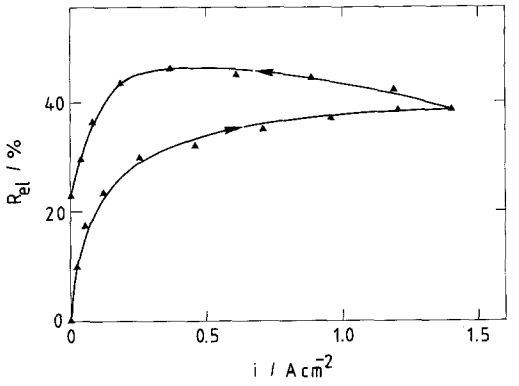

Fig. 5. Change of ohmic resistance, R_{el} (%), versus current density relative to zero current density for increasing (lower curve) and decreasing (upper curve) potential at 1010° C. Anode properties: apparent density, 1.42 g cm^{-3}; baking temperature, 1100° C.

4.2. *Results and discussion*

4.2.1. Ohmic voltage drop. There was appreciable hysteresis between R_{el} recorded during increasing and decreasing potential. As shown in Fig. 5 it increased rapidly with increasing current density up to ~0.2 A cm^{-2} and thereafter it increased much more slowly or remained practically constant. When the potential was lowered, R_{el} kept on increasing until it attained a slight maximum at 0.4–0.5 A cm^{-2} and it then dropped rather abruptly below 0.2 A cm^{-2}. The changes in R_{el} are probably due to shielding of the anode surface by adhering gas bubbles and by gas bubbles rising in the electrolyte. Apparently the shielding levelled off when the current density reached 0.2 A cm^{-2}. A similar conclusion might possibly be drawn from the change of C_{dl} versus potential, as illustrated in Fig. 3.

The relative increase of R_{el} from the value measured at the potential 1.2 V to that of current density = 0.7 A cm^{-2} averaged 10–35%, and showed only a slight tendency to increase with increasing apparent density. The relative increase is far less than suggested by Dewing and van der Kouwe [17]. The absolute values of R_{el} seemed to be dependent on apparent density, and the lowest values were obtained for anodes with high apparent density. The reason for this is not clear. It can hardly be attributed to differences in the conductivity of the anode material itself, since it amounted to only 2–5% of the total resistance. The ohmic voltage drop (IR_{el}) at 0.7 A cm^{-2} is plotted versus apparent density in Fig. 6. The

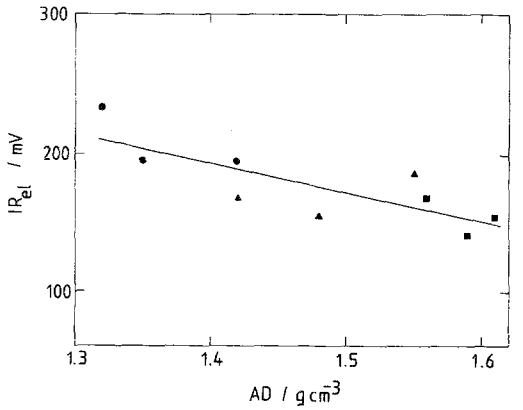

Fig. 6. Ohmic voltage drop (IR_{el}) between anode and reference electrode at 0.7 A cm^{-2} for different baked carbon anodes versus apparent density (AD). Baking temperatures: ●, 970° C; ▲, 1100° C, ■, 1250° C.

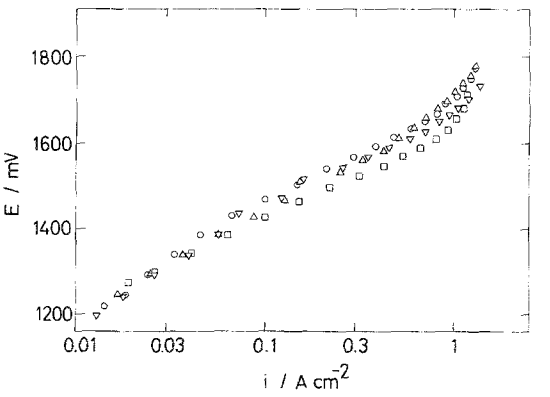

Fig. 8. Polarization potential versus current density at 1010° C for different values of apparent density and baking temperature: ○, 1.42 g cm^{-3}, 970° C; ▽, 1.42 g cm^{-3}, 1100° C; △, 1.55 g cm^{-3}, 1100° C: □, 1.56 g cm^{-3}, 1250° C.

curve indicates that an increase in apparent density by 0.1 g cm^{-3} leads to a 20 mV drop in ohmic voltage. The same trend was observed by Zuca *et al.* [4], but the change was about six times larger.

4.2.2. Potential–current relationship. Despite pre-electrolysis a hysteresis was observed in potential–current plots recorded for increasing and decreasing potential, as shown in Fig. 7. The curves were almost parallel, the descending curve being higher by ~50 mV, except at very low current densities where the slope of the latter curve was much steeper. Such hysteresis is not uncommon for carbon, and it may be attributed either to a continuous change of surface properties and area as a result of the oxidation process [1] and/or to a change in the composition of the anode gas [18]. In general the ascending curves were considered to be the most reliable and these data are presented in the following figures. Fig. 8 shows plots for four different carbon anodes baked at three different temperatures (970, 1100 and 1250° C). The curves can be divided into three segments which were found for almost all samples. The two lower segments were approximately linear. The slope of the first segment in the current density range of 0.01 to ~0.1 A cm^{-2} varied from 0.20 to 0.44 V per decade and that for the range 0.1 to ~0.5 A cm^{-2} varied from 0.18 to 0.24 V per decade. In the third segment (> 0.5 A cm^{-2}) the curves tended to bend upwards. The position of the segments was independent of apparent density and baking temperature. In all cases the slope of the first segment of the plots was higher than that of the second. This difference was particularly pronounced on descending curves, as illustrated in Fig. 7.

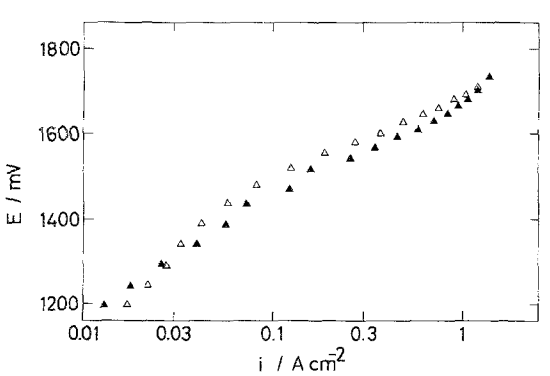

Fig. 7. Polarization potential (referred to aluminium) versus current density for baked carbon anodes at 1010° C. Apparent density, 1.42 g cm^{-3}; baking temperature, 1100° C. ▲, Increasing potential; △, decreasing potential.

In most of the previously published papers [1] the overpotential data were presented as one linear Tafel type of plot ($\eta = a + b \log i$) within the approximate range 0.05–0.7 A cm^{-2} with slopes (b) varying from 0.12 to 0.6 V per decade, although rarely exceeding 0.35 V per decade. A few works performed at current densities below 0.05 A cm^{-2} have given results similar to the present data, i.e. a steeper slope in this range [19, 20]. For graphite anodes Piontelli *et al.* [19] reported slopes of 0.27–0.33 V per decade depending on the alumina concentration at

0.005–0.1 A cm^{-2}, and an almost horizontal segment (0.04 V per decade) at 0.1–0.5 A cm^{-2}. Paunovic [20] found two slopes for graphite anodes of 0.29 V per decade below 0.1 A cm^{-2} and 0.14 V per decade above 0.1 A cm^{-2}. This behaviour was ascribed to a change over of the rate-determining step for the reaction sequence

$$O^{2-} + C \rightarrow CO_{ads} + 2e \quad (2)$$

and

$$CO_{ads} + O^{2-} \rightarrow CO_2 + 2e \quad (3)$$

Dewing and van der Kouwe [17] used baked carbon anodes of the Soderberg type. A slope of 0.29 V per decade was found in the range 0.04–8 A cm^{-2} except for a discontinuity between 0.2 and 0.5 A cm^{-2} where the slope was < 0.1 V per decade.

The change of slope at 0.05–0.1 A cm^{-2} may possibly be associated with a change in the reaction mechanism. It is known that the content of CO evolved increases as the current density is lowered, and it is appreciable below 0.05 A cm^{-2} [1]. This behaviour can result from a shift in the charge transfer control as suggested by Paunovic [20] (Equations 2 and 3), but chemical reaction control cannot be ruled out either. However, any further discussion of the slopes below 0.05–0.1 A cm^{-2} is not warranted since the overpotential is so low in this range that the assumption on which the semi-logarithmic plot is based is not valid [21]. The upward bend of the curve at above 0.5–0.6 A cm^{-2} (Fig. 8) agrees well with results of earlier works on graphite [4, 17, 18, 22, 23] as well as on baked carbon [4, 17, 22–24]. This break has been associated with concentration overvoltage [18] or accumulation of gas bubbles [23].

The current density required to attain an overpotential of 0.5 V was calculated by subtracting the standard e.m.f. ($-E^0 = 1.162$ V at 1010° C) for reaction 1 from the polarization potential. No correlation between this current density and C_{dl} was found. In Fig. 9 it is plotted versus apparent density, and no distinct trend is discernible. This behaviour appears to be in conflict with the conclusions of Zuca *et al.* [4] and Sverdlin *et al.* [3], although direct comparison of the results is difficult. Zuca *et al.* [4] reported that the current density required to reach certain overpotentials showed a marked and linear increase

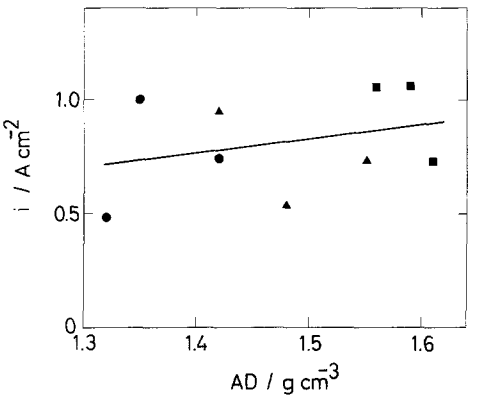

Fig. 9. Current density required to reach 0.5 V overpotential on baked carbon anodes at 1010° C as a function of apparent density (AD). Baking temperatures: ●, 970° C; ▲, 1100° C; ■, 1250° C.

with increasing microporosity for anodes with apparent densities in the range 1.48–1.57 g cm^{-3}. Sverdlin *et al.* [3] found a marked decrease of the counter e.m.f. with increasing volume of transporting pores (i.e. open pores), as mentioned in the introduction. Also, in other systems the relationship between porosity and overvoltage is not clean-cut for gas-evolving electrodes. Thus, for chlorine evolution on RuO_2 in aqueous systems the current has been found to be independent of the true surface area [25].

On the basis of the C_{dl} results a reference value of 220 μF cm^{-2} was chosen, and the current densities were recalculated assuming that the working surface area is proportional to C_{dl}. The following equation was used:

$$i_c = i_g \left(\frac{220}{C_{dl}} \right) \quad (4)$$

where i_c is the corrected current density and i_g is the nominal current density based on the geometrical surface area. The reference value of 220 μF cm^{-2} represented an average for the most dense uniform carbons baked at 1250° C, being at the same time the lowest value common to the materials baked at all three tested baking temperatures. The C_{dl} of vitreous carbon was deemed to be too far below the range of industrial anodes to be suitable as a reference. If the whole wetted area is assumed to be equally accessible, these corrected data should reflect only the influence of the reactivity of the carbon anodes. This assumption implies that the

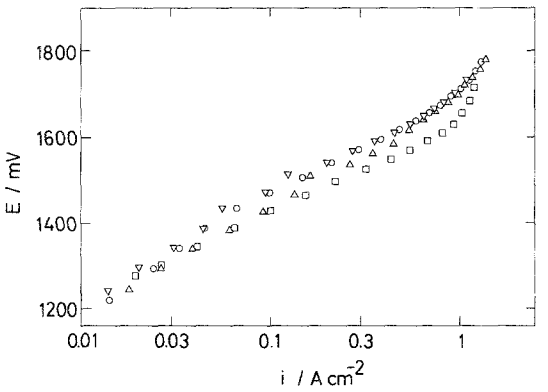

Fig. 10. Polarization potential of baked carbon anodes versus corrected current densities (see text). ○, 1.42 g cm^{-3}, 970° C; ▽, 1.42 g cm^{-3}, 1100° C; △, 1.55 g cm^{-3}, 1100° C; □, 1.56 g cm^{-3}, 1250° C.

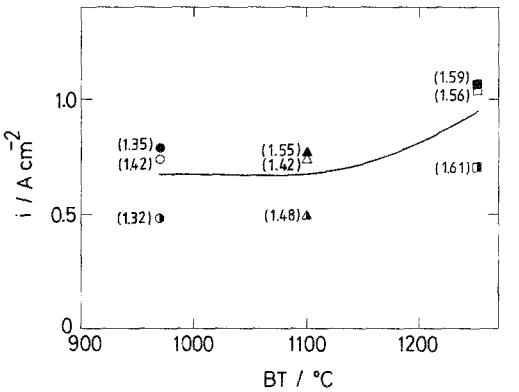

Fig. 11. Corrected current density (see text) required to reach 0.5 V overpotential versus baking temperature (BT). Values of apparent density are given in parentheses.

reactivity is independent of the porosity or the apparent density of the samples. The original results given in Fig. 8 are replotted in Fig. 10 after this correction. Tafel coefficients for the intermediate segment of the curves for current densities in the range 0.1–0.5 A cm^{-2} are listed in Table 3. The data shown in Fig. 9 were recalculated in the same way and plotted in Fig. 11 versus baking temperature.

The correction for surface area slightly reduced the scatter of the Tafel plots. It appears from Figs 10 and 11 that within the temperature range 970–1100° C the baking temperature had no effect on overpotential, while anodes baked at 1250° C showed slightly lower overpotentials. The latter observation may seem to be in conflict with the results of Haupin [26] who found that an increase in baking temperatures within the range 900–1100° C caused a slight increase in overpotential. It may also seem to be in conflict with the well-established fact [1] that graphite gives higher overpotential than baked carbon, which has a disordered carbon structure. The carbon materials used in the present investigation were also subjected to carbon consumption tests [6]. The excess carbon consumption with respect to reaction 1 decreased markedly with increasing baking temperature. The decrease in excess consumption due to the Boudouard reaction ($CO_2 + C = 2CO$) was related to the fact that the pore volume in the 0.5–15 μm size range decreased with increasing baking temperature. A baking temperature of 1250° C is apparently too low to affect the surface reactivity of the carbon material significantly. Dewing and van der Kouwe [17] found that the calcination temperature of the petroleum coke (1200–1400° C) had practically no effect on the overpotential of Soderberg-type anodes.

The present results do not warrant any detailed discussion on the reaction mechanism beyond that which has already been published on the subject. However, the results demonstrate the need for accurate determination of the ohmic resistance as a function of the electrolysis current density, and they also demonstrate the usefulness of the concept of wetted surface area. In view of the above results it appears that an increase of baking temperature of carbon anodes to 1250° C is beneficial since it reduces

Table 3. Tafel coefficients in the current density range 0.1–0.5 A cm^{-2} (see text for corrected current densities)

Baking temperature (° C)	*Apparent density (g cm^{-3})*	*Tafel coefficients*	
		a *(V)*	b *(V per decade)*
970	1.32	0.57	0.22
	1.35	0.52	0.23
	1.42	0.53	0.22
1100	1.42	0.52	0.19
	1.48	0.55	0.20
	1.55	0.52	0.24
1250	1.56	0.47	0.20
	1.59	0.46	0.21
	1.61	0.50	0.18

the ohmic voltage drop and also to a minor extent the anodic polarization. These effects combined with lower excess carbon consumption [6] should result in better performance of anodes baked at elevated temperatures.

Acknowledgements

One of the authors (SJ) gratefully acknowledges a fellowship from The Royal Norwegian Council for Scientific and Industrial Research, which also supported the experimental work. The authors are indebted to Drs T. Naterstad and T. Foosnæs from Hydro Aluminium, Carbon R & D, Ardalstangen, for their cooperation in preparing the samples. Without their help this investigation would not have been possible.

References

[1] K. Grjotheim, C. Krohn, M. Malinovsky, K. Matiasovsky and J. Thonstad, 'Aluminium Electrolysis, Fundamentals of the Hall-Heroult Process', 2nd edn, Aluminium-Verlag, Dusseldorf (1982).
[2] D. Dumas and J. Brenet, *Rev. Roum. Chim.* **14** (1969) 1339.
[3] V. A. Sverdlin, B. S. Dyblin and M. M. Vetyukov, *Sov. J. Non-Ferrous Met.* **17** (1976) (11) 43.
[4] S. Zuca, C. Herdlicka and M. Terzi, *Electrochim. Acta* **25** (1980) 211.
[5] S. Zuca, I. Galasiu and M. Terzi, Proceedings, 4th Czechoslovak Al Symposium Dom techniky ČSVTS, Baska Bystrica, (1980) p. 184.
[6] T. Muftuoglu, J. Thonstad and H. A. Øye, 'Light Metals 1986', (edited by R. E. Miller), Metallurgical Society of AIME, Warrendale (1986) p. 557.
[7] J. Thonstad, *J. Appl. Electrochem.* **2** (1973) 315.
[8] J. Thonstad, *Electrochim. Acta* **15** (1970) 1581.
[9] S. Jarek and Z. Orman, *Electrochim. Acta* **30** (1985) 342.
[10] S. I. Rempel, 'Anodic Processes in Electrolytic Production of Aluminium', Metallurgizdat, Sverdlovsk (1961) (in Russian).
[11] P. Drossbach and T. Hashino, *J. Electrochem. Soc. Jap.* **33** (1965) 229.
[12] R. Holze and W. Vielstich, *J. Electrochem. Soc.* **131** (1984) 2298.
[13] M. M. Vetyukov and F. Akgva, *Sov. J. Non-Ferrous Met.* **11** (1970) (12) 30.
[14] V. A. Cammarota and D. Schlain, US Bureau of Mines, Report Inv. No. 7370 (1970).
[15] J. Thonstad, *Travaux ICSOBA* **10** (1973) 75.
[16] R. Farr-Wharton, B. J. Welch, R. C. Hannah, R. Dorin and H. J. Gardner, *Electrochim. Acta* **25** (1980) 217.
[17] E. Dewing and E. Th. van der Kouwe, *J. Electrochem. Soc.* **122** (1975) 358.
[18] N. E. Richards and B. J. Welch, Electrochemistry, Proceedings, 1st Australian Conf., Pergamon Press (1964) p. 901.
[19] R. Piontelli, B. Mazza and P. Pedeferri, *Electrochim. Acta* **10** (1965) 117.
[20] M. Paunovic, *Electrochim. Metal.* **3** (1968) 373.
[21] K. Vetter, 'Electrochemical Kinetics', Academic Press, New York (1967).
[22] M. M. Vetyukov and A. Baraka, Paper presented at Franco-Russian symposium on aluminium electrolysis, Leningrad (1968).
[23] J. Thonstad, *Electrochim. Acta* **15** (1970) 1569.
[24] M. M. Vetyukov and R. G. Chuvilyaev, *Izv. Vyssh. Ucheb. Zaved. Tsvet. Met.* **8** (1965) (2) 65.
[25] S. Trasatti, *Electrochim. Acta* **32** (1987) 369.
[26] W. Haupin, *J. Electrochim. Soc.* **103** (1956) 174.